

Nonlocal homogenization model for a periodic array of ϵ -negative rods

Mário G. Silveirinha*

Departamento de Eng. Electrotécnica da Universidade de Coimbra, Instituto de Telecomunicações, Pólo II, 3030 Coimbra, Portugal

(Received 5 February 2006; published 26 April 2006)

We propose an effective permittivity model to homogenize an array of long thin ϵ -negative rods arranged in a periodic lattice. It is proven that the effect of spatial dispersion in this electromagnetic crystal cannot be neglected, and that the medium supports dispersionless modes that guide the energy along the rod axes. It is suggested that this effect may be used to achieve subwavelength imaging at the infrared and optical domains. The reflection problem is studied in detail for the case in which the rods are parallel to the interfaces. Full wave numerical simulations demonstrate the validity and accuracy of the new model.

DOI: [10.1103/PhysRevE.73.046612](https://doi.org/10.1103/PhysRevE.73.046612)

PACS number(s): 42.70.Qs, 78.20.Bh, 41.20.Jb, 77.22.-d

I. INTRODUCTION

In recent years there has been a lot of interest in the propagation of electromagnetic waves in artificial materials, and particularly in materials with a negative index of refraction [1,2]. The research has been mainly driven by the possibility of using these materials to miniaturize several devices and waveguides, and develop “perfect lenses” that are able to focus electromagnetic radiation with subwavelength resolution [3]. Recently, a different approach to achieve subwavelength resolution was proposed in [4] and demonstrated experimentally in [5]. In [5] the idea is to use an artificial material formed by an array of perfectly conducting wires (wire medium) to guide the waves from the input plane to the output plane, and then reconstruct the image “pixel by pixel,” exploring a Fabry-Perot resonance that in the wire medium occurs simultaneously for all the spatial harmonics. The resolution of this transmission device is only limited by the lattice constant, i.e., by the spacing between the wires. The problem with the configuration studied in [5] is that it is limited to the microwave regime because in the optical domain perfect electric conducting materials are not available. Nevertheless, we will suggest in this paper that it may still be possible to use the same concept to achieve subwavelength resolution at the infrared and optical domains, provided ϵ -negative (ENG) rods are used to guide the electromagnetic radiation instead of metallic wires. At the infrared and optical frequencies all metallic materials have permittivity with a negative real part. It is known that their dielectric constant is well represented by the Drude model $\epsilon = 1 - \omega_p^2 / \omega^2$, where ω_p is the plasma frequency (for simplicity the lossless model was considered). Thus, we envision that either silver or gold rods may be used to fabricate transmission devices that are able to propagate the subwavelength information of an image.

With this motivation, we will investigate in this paper the propagation of electromagnetic waves in an artificial medium formed by thin ENG rods (see Fig. 1), and we will show that the structure can be homogenized and described by an effective permittivity tensor provided spatial dispersion is taken

into account. We will show that our homogenization model predicts that the rod medium may support a mode that propagates along the axes of the rods with the same phase velocity, independently of the transverse wave vector. As proven in [4], this is a key property to operate the material in the canalization regime and achieve subwavelength resolution.

Previous works related with the homogenization of ENG rods are discussed next. In [6] the oblique propagation of electromagnetic waves through an array of aligned fibers was examined, and the associated problem of numerical instability was discussed. In [7] a method was proposed to compute analytically the band structure of wire mesh crystals. In [8] a model was proposed to homogenize a medium with metallic rods, but only the on-plane case was considered. In [9] a homogenization model was proposed to characterize a structure similar to the one studied in this paper. It was demonstrated that the artificial material was characterized by spatial dispersion, and that the band structure of the photonic crystal had several branches. However, the results of [9] are restricted to the case in which the permittivity of the rods follows a Drude-type plasma model, and besides that the derived formulas for the effective permittivity are very cumbersome, lead to nonanalytical dispersion characteristics, and more importantly hide the physics of the problem. In this paper, we will derive a simpler and more intuitive model, describe new phenomena, and prove that the new approach can characterize accurately the electrodynamics of the artificial medium.

The homogenization of the wire medium is also closely related to the subject under study. In fact, the case of perfectly conducting wires can be regarded as the limit situation in which the permittivity of the ENG rods is $-\infty$. In [10] a homogenization model was derived for the wire medium, and it was proven that this artificial material suffers from strong spatial dispersion even for very long wavelengths. Later, in [11,12,21], these results were generalized for 2D and 3D lattices of connected and unconnected wires. In [13,14] the reflection problem in a wire medium slab was investigated, and in [15] it was proven that, in general, an additional boundary condition is necessary to determine the scattering parameters.

The paper is organized as follows: First, we will characterize the electric polarizability of a dielectric rod. Then, we will derive the homogenization rudiments necessary to cal-

*Electronic address: mario.silveirinha@co.it.pt

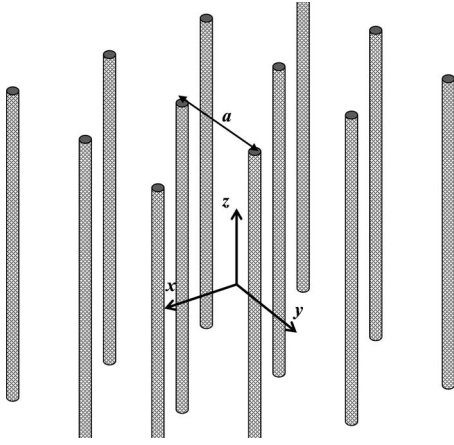


FIG. 1. Medium formed by long thin ENG rods arranged in a square lattice.

culate the effective permittivity of the structure. In Sec. IV, the electromagnetic modes supported by the rod medium are characterized. In Sec. V, we study the reflection problem in a finite slab, assuming that the rods are parallel to the interfaces. The derived results are compared with full wave numerical simulations. Finally, in Sec. VI the conclusions are presented.

In this work we assume that the fields are monochromatic with time variation $e^{+j\omega t}$.

II. POLARIZABILITY OF A DIELECTRIC ROD

Let us consider a ENG rod with radius R and (relative) permittivity $\epsilon = \epsilon(\omega)$. The rod is oriented along the z direction. In this section, we calculate the component α_{zz} of the electric polarizability tensor (actually, since the rod is infinite along z , we are going to calculate the polarizability per unit of length). To this end, we consider that a plane wave with magnetic field along the y direction illuminates the dielectric rod. The wave vector of the incident wave is $\mathbf{k} = (k_x, 0, k_z)$, where $\mathbf{k} \cdot \mathbf{k} = \beta^2$ and $\beta = \omega/c$ is the free-space wave number. The incident electric field along the z direction is

$$E_z^{\text{inc}} = E_0 e^{-jk_x x} e^{-jk_z z} = E_0 e^{-jk_z z} \sum_{n=-\infty}^{\infty} (-j)^{|n|} J_{|n|}(k_{\rho,0} r) e^{jn\varphi}, \quad (1)$$

where J_n is the J Bessel function of first kind and order n , $k_{\rho,0} = \sqrt{\beta^2 - k_z^2}$, and (r, φ) form a system of cylindrical coordinates attached to the rod axis.

The field components along z can be expanded into cylindrical harmonics. For example,

$$E_z = \begin{cases} \sum_{n=-\infty}^{\infty} a_n J_{|n|}(k_{\rho,m} r) e^{jn\varphi} e^{-jk_z z}, & r < R \\ E_z^{\text{inc}} + \sum_{n=-\infty}^{\infty} b_n H_{|n|}^{(2)}(k_{\rho,0} r) e^{jn\varphi} e^{-jk_z z}, & r > R, \end{cases} \quad (2)$$

where a_n and b_n are the unknown coefficients of the expansion, $H_n^{(2)} = J_n - jY_n$ is the Hankel function of a second kind

and order n , and $k_{\rho,m} = -j\sqrt{k_z^2 - \beta^2 \epsilon}$. The field H_z has a similar expansion.

The transverse fields \mathbf{E}_{\parallel} and \mathbf{H}_{\parallel} (projections into the x - y plane) can be written in terms of E_z and H_z ,

$$\mathbf{E}_{\parallel} = \frac{1}{k_{\rho,i}^2} (-jk_z \nabla_{\parallel} E_z + j\beta \hat{\mathbf{u}}_z \times \nabla_{\parallel} \eta_0 H_z), \quad (3)$$

$$\eta_0 \mathbf{H}_{\parallel} = \frac{1}{k_{\rho,i}^2} (-j\beta \epsilon_i \hat{\mathbf{u}}_z \times \nabla_{\parallel} E_z - jk_z \nabla_{\parallel} \eta_0 H_z). \quad (4)$$

In the above, η_0 is the free-space impedance, $\nabla_{\parallel} = (\frac{\partial}{\partial x}, \frac{\partial}{\partial y}, 0)$, $\epsilon_i = \epsilon$, and $k_{\rho,i} = k_{\rho,m}$ inside the rod, and $\epsilon_i = 1$ and $k_{\rho,i} = k_{\rho,0}$ outside.

The unknown coefficients can be calculated by imposing the continuity of the tangential electromagnetic fields (i.e., E_z , E_{φ} , H_z , H_{φ}) at the interface $r=R$.

The (z component of the) electric dipole moment (per unit of length) is given by

$$\frac{p_z}{\epsilon_0} = (\epsilon - 1) \int_{r \leq R} E_z dS = (\epsilon - 1) 2\pi R a_0 \frac{J_1(k_{\rho,m} R)}{k_{\rho,m}} e^{-jk_z z} \quad (5)$$

and so the polarizability per unit of length is

$$\alpha_{zz} = \frac{p_z}{\epsilon_0 E^{\text{inc}}|_{x=y=0}} = (\epsilon - 1) 2\pi R \frac{a_0 J_1(k_{\rho,m} R)}{E_0 k_{\rho,m}}. \quad (6)$$

This result shows that a_0 is the unique coefficient required to calculate the polarizability. Since Maxwell equations are separable in cylindrical coordinates, to calculate a_0 it is sufficient to impose the boundary conditions to the terms associated with the cylindrical harmonic $n=0$. It can be easily verified that the $n=0$ term of the magnetic field H_z vanishes (this happens because $H_z^{\text{inc}} = 0$ and $\frac{\partial}{\partial \varphi} = 0$ for the $n=0$ harmonic). Thus, only the tangential components E_z and H_{φ} have nontrivial $n=0$ coefficients. Using (1)-(2) in (3)-(4), and imposing the continuity of the tangential fields, we find that

$$a_0 J_0(k_{\rho,m} R) = b_0 H_0^{(2)}(k_{\rho,0} R) + E_0 J_0(k_{\rho,0} R), \quad (7)$$

$$a_0 \frac{\epsilon}{k_{\rho,m}} J_0'(k_{\rho,m} R) = b_0 \frac{1}{k_{\rho,0}} H_0'^{(2)}(k_{\rho,0} R) + \frac{1}{k_{\rho,0}} E_0 J_0'(k_{\rho,0} R), \quad (8)$$

where the prime “'” denotes the derivative of a function. Solving for a_0 we readily obtain

$$a_0^{-1} = j \frac{\pi k_{\rho,0} R}{2E_0} \left[J_0(k_{\rho,m} R) H_0'^{(2)}(k_{\rho,0} R) - \frac{\epsilon k_{\rho,0}}{k_{\rho,m}} J_0'(k_{\rho,m} R) \times H_0^{(2)}(k_{\rho,0} R) \right]. \quad (9)$$

Substituting this result in Eq. (6), we obtain the desired electric polarizability

$$\alpha_{zz}^{-1} = j \frac{k_{\rho,0}}{4} \frac{1}{\epsilon - 1} \left[-k_{\rho,m} \frac{J_0(k_{\rho,m}R)}{J_1(k_{\rho,m}R)} H_1^{(2)}(k_{\rho,0}R) + \epsilon k_{\rho,0} \right. \\ \left. \times H_0^{(2)}(k_{\rho,0}R) \right]. \quad (10)$$

In this work, we consider that the radius of the rods is always much smaller than the wavelength, or equivalently, $Rk_{\rho,0} \ll 1$. In these circumstances, Eq. (10) simplifies to

$$\alpha_{zz}^{-1} \approx \frac{1}{(\epsilon - 1)\pi R^2} \left\{ 1 + j \frac{\pi}{4} (\epsilon - 1) (k_{\rho,0}R)^2 \right. \\ \left. + \frac{1}{2} (\epsilon - 1) \left[C + \log\left(\frac{k_{\rho,0}R}{2}\right) \right] (k_{\rho,0}R)^2 \right\}, \quad (11)$$

where C is the Euler constant. It is important to note that because the rods are infinitely long, the polarizability depends not only on the frequency of the incoming wave, but also on the wave vector component k_z . If ϵ approaches $-\infty$ the above result reduces to the case of perfectly conducting rods studied in [14].

Proceeding similarly, we can obtain the well-known formula for the electric polarizability (per unit of length) in the transverse plane (x - y plane),

$$\alpha_{xx} = \alpha_{yy} \approx \frac{\epsilon - 1}{\epsilon + 1} 2\pi R^2. \quad (12)$$

Provided the permittivity of the rods is not too close to the resonance $\epsilon = -1$ and the rods are very thin, the polarizability can be neglected in the transverse plane.

III. EFFECTIVE PERMITTIVITY MODEL

In the following, we derive an effective permittivity model for the medium formed by a periodic array of ENG rods. As depicted in Fig. 1, the rods are arranged in a square lattice and the spacing between the rods (lattice constant) is a . As is well known, each electromagnetic (Floquet) mode in a periodic medium can be associated with a wave vector $\mathbf{k} = (k_x, k_y, k_z)$. For convenience, we define $\mathbf{k}_{\parallel} = (k_x, k_y, 0)$.

To compute the effective permittivity we use the mixing formula,

$$\bar{\bar{\epsilon}} = \bar{\bar{\mathbf{I}}} + \frac{1}{A_{\text{cell}}} (\bar{\bar{\alpha}}_e^{-1} - \bar{\bar{\mathbf{C}}}_{\text{int}})^{-1}, \quad (13)$$

where $A_{\text{cell}} = a^2$, $\bar{\bar{\mathbf{I}}}$ is the identity dyadic, the superscript “ -1 ” represents the inverse dyadic, and $\bar{\bar{\mathbf{C}}}_{\text{int}}$ is the interaction dyadic calculated in Appendix B. The mixing formula is derived in Appendix A, and is valid under the condition that the dimensions of the cross section are much smaller than the lattice constant, and that $|\mathbf{k}_{\parallel}|a \ll 2\pi$. As discussed in Appendix A, even though Eq. (13) reminds us of the Clausius-Mossotti formula, things are not so plain because the lattice has some intrinsic dispersion. To keep the readability of the paper the details have been moved to Appendix A.

Next we substitute Eqs. (11) and (12) in Eq. (13). Using Eq. (B4), we find that the effective permittivity in the transverse plane is

$$\epsilon_{xx} = \epsilon_{yy} = 1 + \frac{2}{\frac{1}{f_V} \frac{\epsilon + 1}{\epsilon - 1} - 1}, \quad (14)$$

where $f_V = \pi R^2 / A_{\text{cell}}$ is the volume fraction of the rods. Provided the permittivity of the rods does not satisfy $\epsilon \approx -1$ and the rods are very thin, we can assume that $\epsilon_{xx} = \epsilon_{yy} \approx 1$. For simplicity, we shall assume this situation in the rest of the paper. On the other hand, from Eq. (13) it is clear that

$$\epsilon_{zz} = 1 + \frac{1}{A_{\text{cell}} \alpha_{zz}^{-1} - C_{\text{int},zz}}, \quad (15)$$

where $C_{\text{int},zz}$ is given by Eq. (B7). So, after further simplifications, we obtain that

$$\epsilon_{zz} = 1 + \frac{1}{\frac{1}{(\epsilon - 1)f_V} - \frac{\beta^2 - k_z^2}{\beta_p^2}}, \quad (16)$$

where β_p is the plasma wave number defined consistently with the results of [14] for perfectly conducting wires,

$$(\beta_p a)^2 = \frac{2\pi}{\ln\left(\frac{a}{2\pi R}\right) + \frac{\pi}{6} + \sum_{n=1}^{\infty} \frac{1}{|n|} \frac{2}{e^{2\pi|n|} - 1}} \\ \approx \frac{2\pi}{\ln\left(\frac{a}{2\pi R}\right) + 0.5275}. \quad (17)$$

Note that in general ϵ is a function of frequency. Formula (16) gives the effective permittivity of an array of diluted ENG rods. The first important observation is that the medium is spatially dispersive. Indeed the permittivity depends not only on the frequency $\beta = \omega/c$, but also on the component of the wave vector parallel to the rods. This means that the medium is nonlocal, i.e., in the spatial domain the electric displacement vector and the electric field are related through a spatial convolution rather than by a multiplication. Secondly, we note that if the permittivity of the rods approaches $-\infty$, Eq. (16) reduces to the formula derived in [10] for the wire medium, consistently with the observation made in the introduction of this paper. Finally, if we put $\beta = 0$ and assume on-plane propagation, i.e., $k_z = 0$, the effective permittivity simplifies to $\epsilon_{zz} = 1 + (\epsilon - 1)f_V$, which is the exact formula in the static the limit for nondispersive dielectrics [16]. Thus, very interestingly, formula (16) is in a certain sense the average of these two limit situations. Note that even though in this work our main interest is the analysis of ENG rods, the proposed model is also valid for dielectrics with positive real part of the permittivity. In the next sections, we characterize the electromagnetic modes supported by the rod medium and validate the model with numerical simulations.

IV. CHARACTERIZATION OF THE ELECTROMAGNETIC MODES

It is evident that the waves in the homogenized medium can be decomposed into transverse electric (TE) modes

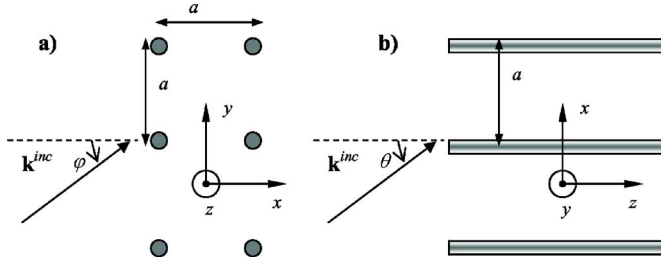


FIG. 2. (Color online) Reflection of a plane wave by a semi-infinite rod medium. (a) The axes of the rods are parallel to the interface. (b) The axes of the rods are normal to the interface.

(electric field is normal to the axes of the ENG rods), and transverse magnetic (TM) modes (magnetic field is normal to the axes of the ENG rods). As explained in the previous section, we shall assume in this paper that $\epsilon_{xx} = \epsilon_{yy} \approx 1$ (i.e., that the rods are very thin, and that the permittivity of rods is not close to $\epsilon \approx -1$). Within this approximation, the TE modes do not interact with the rods, and thus their dispersion characteristic is

$$\beta^2 = k^2 \quad (18)$$

and the associated average electric field is (the propagation factor $e^{-j\mathbf{k}\cdot\mathbf{r}}$ is implicit)

$$\mathbf{E}_{av}^{TE} \propto \frac{\mathbf{k}_{\parallel} \times \hat{\mathbf{u}}_z}{|\mathbf{k}_{\parallel} \times \hat{\mathbf{u}}_z|}. \quad (19)$$

On the other hand, the TM modes satisfy the characteristic equation,

$$k_{\parallel}^2 = \epsilon_{zz}(\beta^2 - k_z^2). \quad (20)$$

The above equation cannot be solved explicitly as a function of β , because the permittivity of the rods is itself a function of β . The corresponding average electric field is (for $k_z \neq 0$)

$$\mathbf{E}_{av}^{TM} \propto \left(\frac{\mathbf{k}_{\parallel}}{\beta} + \frac{\beta^2 - k^2}{\beta^2 \epsilon_{zz} - k^2} \frac{k_z}{\beta} \hat{\mathbf{u}}_z \right). \quad (21)$$

The associated magnetic field can be calculated using Eq. (A2).

To better understand the nature of the TM modes, we then study a reflection problem. Let us consider a semi-infinite rod medium illuminated from the air side with a plane wave. We analyze two different geometries, as depicted in Fig. 2.

First, let us suppose that the axes of the rods are parallel to the interface $x=0$ [Fig. 2(a)]. The incident wave vector is $\mathbf{k}^{inc} = (-j\gamma_0, k_y, k_z)$ with $\gamma_0 = \sqrt{k_y^2 + k_z^2 - \beta^2}$. It is well known that the component of the incident wave vector parallel to the interface, $(0, k_y, k_z)$, is preserved. In this case only one TM mode is excited in the artificial medium (besides the TE mode). Indeed, from Eq. (20) the component k_x of the wave vector inside the rod medium is given by

$$k_{x,rod}^2 = -k_y^2 + \epsilon_{zz}(\beta^2 - k_z^2). \quad (22)$$

Notice that the right-hand side of the above equation only depends on the geometry and parameters of the medium, on the wave number β of the incident wave, and on the compo-

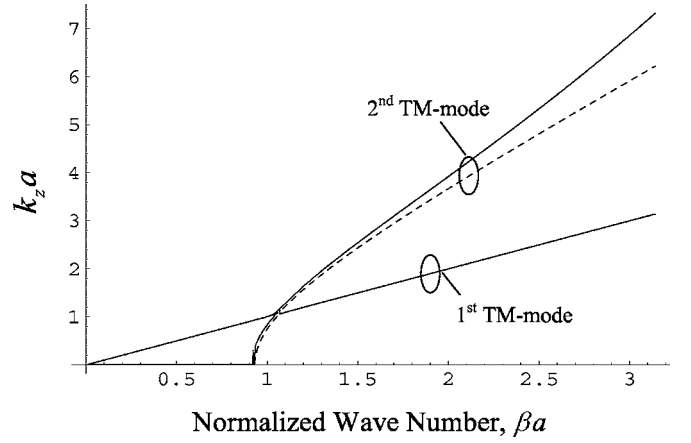


FIG. 3. Plot of k_z as a function of normalized frequency βa , for $R=0.05a$ and $k_{\parallel}=0$. The permittivity ϵ follows a Drude-type model (see the text). The solid line represents the “exact” result, whereas the dashed line represents the results calculated with the proposed model.

nents of the incident wave vector that are preserved $(0, k_y, k_z)$.

Next suppose that the rods are normal to the interface $z=0$ [Fig. 2(b)]. The incident wave vector is now $\mathbf{k}^{inc} = (k_x, k_y, -j\gamma_0)$ with $\gamma_0 = \sqrt{k_x^2 + k_y^2 - \beta^2}$. The interesting thing is that for this configuration two TM modes can be excited inside the rod medium. Indeed, since $\mathbf{k}_{\parallel} = (k_x, k_y, 0)$ to find the excited electromagnetic modes one needs to solve Eq. (20) for k_z . Straightforward calculations, using Eq. (16), show that

$$k_z^2 = \beta^2 - \frac{1}{2}(\beta_p^2 + k_{\parallel}^2 - \beta_c^2 \pm \sqrt{(\beta_p^2 + k_{\parallel}^2 - \beta_c^2)^2 + 4\beta_c^2 k_{\parallel}^2}), \quad (23)$$

where we defined the parameter $\beta_c = \beta_c(\omega)$ as,

$$\beta_c^2 = -\frac{\beta_p^2}{(\epsilon(\omega) - 1)f_V}. \quad (24)$$

Note that provided the permittivity of the rods is less than the permittivity of the host medium, β_c is a positive real number (with the same unities as β ; for simplicity the rods are assumed lossless, otherwise β_c becomes a complex number). Also, β_c is in general a function of frequency since ϵ also is. From Eq. (23) it is seen that there are two different solutions for k_z , and hence two TM modes, besides the TE mode, can propagate inside the artificial medium. This phenomenon is a manifestation of spatial dispersion, and is also characteristic of the wire medium [10]. We also note that the average electric field for both TM modes is calculated using Eq. (21).

To illustrate the discussion, we plot in Fig. 3, k_z as a function of normalized frequency βa for the parameters $R=0.05a$, $k_{\parallel}=0$, assuming that the permittivity follows the Drude model $\epsilon = 1 - \beta_m^2/\beta^2$ with (normalized) plasma wave number $\beta_m a = 12.0$. The dashed line curve represents the results calculated using Eq. (23). The solid line curve corresponds to the data calculated by substituting Eq. (10) in Eq.

(15) (with no approximations) and calculating $C_{\text{int},zz}$ using Eq. (B5) with $\mathbf{r}=\mathbf{r}'=\mathbf{0}$, but without making any assumptions with respect to $\mathbf{k}_{\parallel}a$ being negligible. Hence, the permittivity becomes a function of not only β and k_z , but also of the other components of the wave vector. The permittivity function obtained in this way is substituted in Eq. (20), and the corresponding equation is solved numerically. A similar procedure was used in [9,14], and so further details are omitted here. These results can be regarded as “exact” within the thin rod approximation. As seen in Fig. 3, the agreement for the first TM mode is always excellent. On the other hand, the second TM mode is not so accurately predicted for relatively small wavelengths. The reason is twofold. The first reason is that for larger frequencies the long wavelength limit approximation is not so accurate. The second reason will be discussed later. Figure 3 shows that for $k_{\parallel}=0$ one of the electromagnetic modes propagates with the speed of light. It is also important to refer that for very low frequencies one of the TM modes is cut-off (complex imaginary propagation constant). This is because the ENG rods behave as perfect conductors in the static limit (when the permittivity follows the Drude model).

To give further insight about the TM modes, let us study different limit situations. First, suppose that at some frequency $\beta_c(\omega) \ll \beta_p$, i.e., the permittivity of the rods is very large in absolute value. In this case, Eq. (23) reveals that one of the modes has the dispersion characteristic $k_z^2 = \beta^2$, and that the other mode has the dispersion $k_z^2 = \beta^2 - \beta_p^2 - k_{\parallel}^2$. The former mode can be readily identified with the well-known transverse electromagnetic (TEM) dispersionless mode of the wire medium (perfectly conducting wires), while the latter is the TM mode of the wire medium.

Consider now the case $\mathbf{k}_{\parallel} \approx \mathbf{0}$, i.e., paraxial incidence. Using a Taylor expansion we obtain

$$k_z^2 \approx \beta^2 + \frac{k_{\parallel}^2}{2} \left(-1 \pm \frac{\beta_c^2 + \beta_p^2}{\beta_c^2 - \beta_p^2} \right) + \begin{cases} \beta_c^2 - \beta_p^2 \\ 0 \end{cases}. \quad (25)$$

The above formula shows that if either $\beta_c(\omega) \ll \beta_p$ or $\beta_c(\omega) \gg \beta_p$, one of the modes becomes dispersionless with respect to \mathbf{k}_{\parallel} (i.e., the coefficient associated with k_{\parallel}^2 vanishes). The former case was already discussed. As to the latter case, the pertinent mode has dispersion $k_z^2 \approx \beta^2 + \beta_c^2$. But this implies that $k_z > \beta$ and thus this mode is a surface wave guided along the rods. In [17] it was proved that a ENG rod is able to support tightly bounded surface modes that propagate electromagnetic energy with subwavelength beam radius. For metallic materials the surface modes are surface plasmon polaritons. It was shown that the energy becomes more confined to the vicinity of the dielectric waveguide when the effective index of refraction $n_{\text{eff}} = k_z/\beta$ increases. This important result justifies why in the rod medium one of the TM modes becomes independent of \mathbf{k}_{\parallel} . In fact, when $\beta_c(\omega) \gg \beta_p$ each guided mode is confined to a small vicinity of the respective ENG rod, there is no interaction or coupling between the rods, and consequently one of the TM modes becomes dispersionless. As referred to before, when $\beta_c(\omega) \ll \beta_p$ there is also a quasi-TEM dispersionless mode. However this mode is qualitatively very different

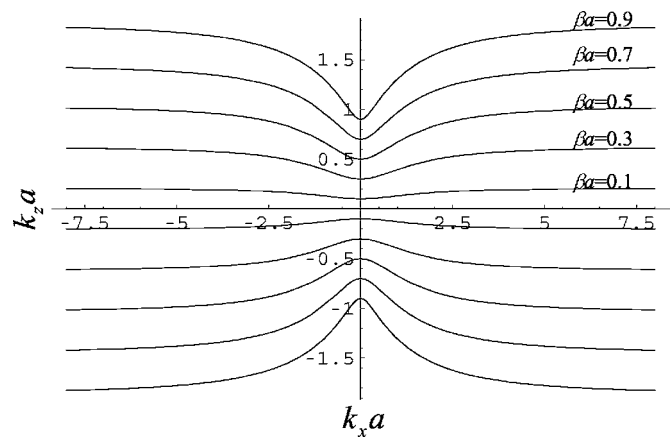


FIG. 4. Plot of k_z as a function of $k_x a$ for $R=0.05a$ and $k_y=0$. Contours $\beta a=0.1, 0.3, 0.5, 0.7, 0.9$ for the TM modes. The permittivity ϵ follows a Drude-type model (see the text).

from the mode that arises when $\beta_c(\omega) \gg \beta_p$. Indeed, while in the latter case the energy is propagated tightly bounded to the ENG rods, in the TEM mode case the field energy is distributed more or less uniformly by the whole volume. As discussed in the Introduction, the dispersionless modes may be used to canalize the electromagnetic radiation through the rod medium and achieve subwavelength imaging. A detailed analysis of this topic is out of the scope of the present paper, and will be reported elsewhere. We also refer that the other TM mode, still assuming that $\beta_c(\omega) \gg \beta_p$, has to a first approximation the dispersion characteristic $k_z^2 \approx \beta^2 - k_{\parallel}^2$, i.e., approximately the same dispersion as the TE mode.

In Figs. 4 and 5, k_z is plotted as a function of k_x for $R=0.05a$ and several different values of the normalized frequency βa (the permittivity of the rods follows the same Drude model as before). For convenience we show the results in two different figures. For very long wavelengths $\beta_c(\omega) \ll \beta_p$, and consequently one of the modes is cutoff. The dispersion of the other mode (shown in Fig. 4) becomes increasingly flat as the frequency (and consequently β_c) decreases. Note that from Eq. (24) and assuming a Drude type model, β_c increases monotonically with the frequency.

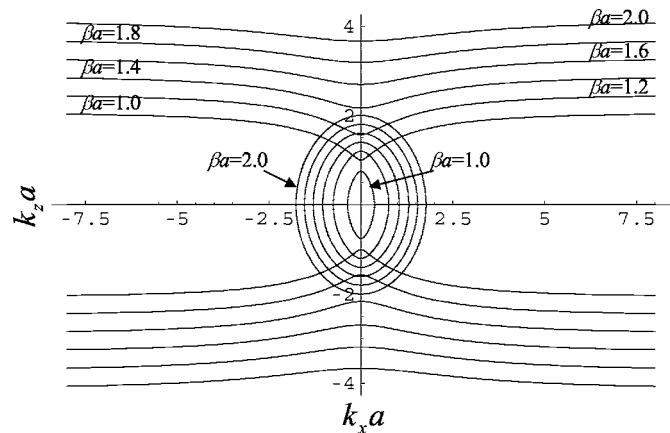


FIG. 5. Plot of k_z as a function of $k_x a$ for $R=0.05a$ and $k_y=0$. Contours $\beta a=1.0, 1.2, 1.4, 1.6, 1.8, 2.0$ for the TM modes. The permittivity ϵ follows a Drude-type model (see the text).

At some point, as the frequency increases, the TM mode that was cutoff starts to propagate. In this case (Fig. 5), for each fixed frequency there are two different contours, i.e., two propagating TM modes. As the frequency increases even more, β_c becomes comparable or larger than β_p , and the band structure of one of the TM modes becomes practically flat, consistently with the fact that the energy propagated by this mode is tightly confined to the vicinity of the ENG rods.

In Figs. 4 and 5 it can also be seen that around $k_{\parallel} \approx 0$ the wave normal contours of one of the modes are to some extent hyperbolic. In fact, using Eq. (25) it can be easily checked that one of the modes has a dispersion characteristic such that the signs of the coefficients associated with k_{\parallel}^2 and k_z^2 are symmetric. This property is more important for frequencies such that $\beta_c(\omega) \approx \beta_p$. Note that if the medium was anisotropic, with no spatial dispersion, and negative permittivity along the z direction the contours would also be hyperbolic. It is well known that hyperbolic contours may originate negative refraction at an interface.

It is also important to refer that in the limit $\varepsilon \rightarrow 1$, the ratio $\beta_c(\omega)/\beta_p$ becomes infinitely large [see Eq. (24)] and consequently k_z/β is also infinitely large. This means that in these circumstances the localized TM mode either cannot be excited by an incoming wave, or if it is excited it is killed by losses. Thus, only the other TM mode, with dispersion $k_z^2 \approx \beta^2 - k_{\parallel}^2$, will propagate. This is consistent with the fact that as $\varepsilon \rightarrow 1$ the medium shall have the same properties as free space.

To conclude this section, we will discuss the scope of application of the permittivity model (16). We remember that the results were derived for thin rods, $R \ll a$, and under the assumption that $|k_{p,0}|a \ll \pi$ and $\beta a \ll \pi$. In general the modes that propagate in the long wavelength limit satisfy the previous conditions without problems. However, there is one exception with the problem at hand. In fact, when $\beta_c(\omega) \gg \beta_p$ the radial constant $k_{p,0}$ becomes complex imaginary for the TM mode associated with the surface mode (surface plasmon). As discussed in [17], when the beam radius is sub-wavelength the effective index of refraction $n_{\text{eff}} = k_z/\beta$ becomes very large, and in that case the condition $|k_{p,0}|a \ll \pi$ may not be observed. This situation affects the accuracy of our model when $\beta_c(\omega) \gg \beta_p$. Indeed, the error in the TM mode associated with the surface mode becomes non-negligible in this situation. The other TM mode is still accurately predicted. This result justifies deterioration of the agreement in Fig. 3, as the frequency (and consequently, for the Drude Model, also β_c) increases.

Fortunately, it is easy to solve this problem. In fact, when $\beta_c(\omega) \gg \beta_p$ the dispersion characteristic of the pertinent TM mode is essentially the same as the dispersion characteristic of the guided mode supported by a single ENG rod. This dispersion characteristic is determined in [17], and is equivalent to the condition $\alpha_{zz}^{-1} = 0$, where α_{zz}^{-1} is given by Eq. (10). Thus, to summarize our findings, the TM modes can be accurately calculated using Eq. (23), except when $\beta_c(\omega) \gg \beta_p$ which yields less accurate results for the mode with higher k_z . In this case the corresponding TM mode is dispersionless, and follows the same characteristic as the guided mode supported by a single dielectric rod.

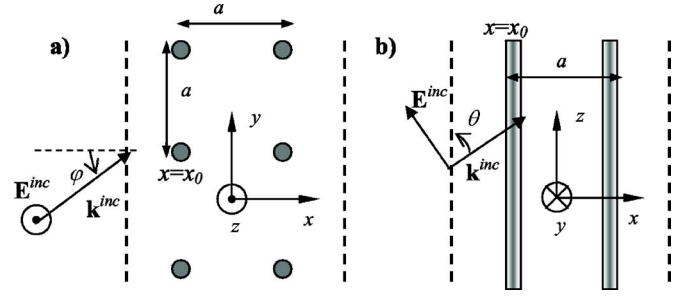


FIG. 6. (Color online) A plane wave illuminates a slab of the rod medium ($N_L=2$). The rods are parallel to the plane $x=0$. (a) $k_z=0$. (b) $k_y=0$.

V. THE REFLECTION PROBLEM WITH RODS PARALLEL TO THE INTERFACES

To further validate the proposed permittivity model, we will study the reflection of electromagnetic waves by a rod medium slab with finite thickness. We will suppose that the rods are parallel to the interface (see Fig. 6). The slab consists of N_L layers of rods. The structure is periodic in y and z , and the dielectric rods stand in free space. The interfaces $x = x'_L$ and $x = x'_R = x'_L + N_L a$ are represented by the dashed lines (since the rods stand in air the definition of the interfaces is a bit ambiguous; this will be discussed below with more detail). The rods in the leftmost layer are in the plane $x = x_0$.

As discussed in the previous section, when the rods are parallel to the interface, Eq. (22) has only one solution for k_x^2 . For simplicity, we will restrict our attention to the case in which either $k_z=0$ [Fig. 6(a)] or $k_y=0$ [Fig. 6(b)]. For these particular geometries, an incident plane wave polarized as depicted in Fig. 6 can only excite the TM mode inside the rod medium. As is well known [18], in the general case where k_y and k_z are simultaneously different from zero, both the TM and TE modes are excited (the medium is birefringent). Apart from the more heavy notation, the general case poses no additional difficulties.

Using Eqs. (A2), (21), and (22), and matching the tangential components of the electric and magnetic fields at the interfaces, we find that the reflection coefficient referred to the plane $x = x'_L$ is given by

$$\rho = \frac{\tanh(\gamma_m d)(\gamma_0^2 - \gamma_m^2)}{2\gamma_0\gamma_m + \tanh(\gamma_m d)(\gamma_0^2 + \gamma_m^2)}, \quad (26)$$

$$\rho = \frac{\tanh(\gamma_m d)(\varepsilon^2\gamma_0^2 - \gamma_m^2)}{2\varepsilon\gamma_0\gamma_m + \tanh(\gamma_m d)(\varepsilon^2\gamma_0^2 + \gamma_m^2)}, \quad (27)$$

where $d = N_L a$ is the thickness of the slab, $\gamma_m = jk_{x,\text{rod}}$, $\gamma_0 = \sqrt{k_y^2 + k_z^2 - \beta^2}$, and Eq. (26) corresponds to Fig. 6(a) with $k_z = 0$, and Eq. (27) corresponds to Fig. 6(b) with $k_y = 0$.

Next, in order to demonstrate the accuracy of the theoretical results, the analytical model is tested against full wave data computed with the periodic moment method (MoM) [19]. In the first example we consider that $R = 0.05a$, and $\varepsilon = -30.0$ at $\beta a = 1.0$ (for simplicity, losses are neglected). A plane wave polarized as depicted in Fig. 6(a) illuminates five layers of rods ($N_L = 5$). The amplitude of the reflection coef-

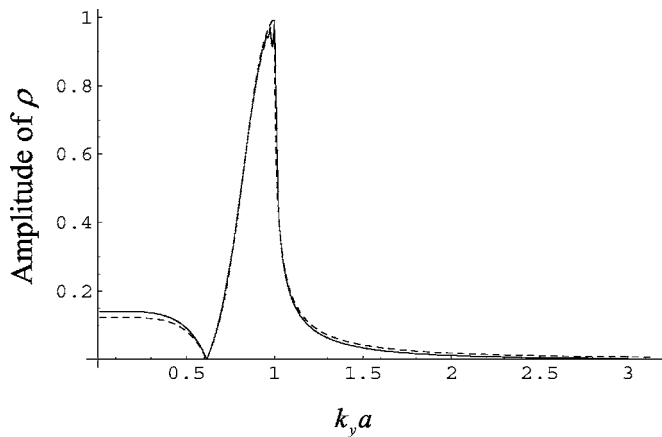


FIG. 7. Reflection coefficient as a function of the wave vector component parallel to the interface. The slab consists of $N_L=5$ layers, and the rods have $R=0.05a$, and $\epsilon=-30$ at $\beta a=1.0$. The solid line represents the full wave MoM data, and the dashed line represents the data obtained using the analytical model.

cient is depicted in Fig. 7 as a function of $k_y a$. Note that the angle of incidence φ is such that $\sin \varphi = k_y / \beta$. For $k_y > \beta$ the incident wave is evanescent. The solid line represents the MoM full wave data. The dashed line represents the results computed using the proposed permittivity model [formula (26)]. It is seen that the agreement between the two sets of data is good. Similar agreement is obtained for the phase of the reflection coefficient and for the transmission coefficient. The previous results also demonstrate that the homogenization model is useful to study not only incident propagating plane waves, but also part of the evanescent spectrum.

As noted before, since the rods stand in free space the position of the interfaces and thickness of the slab are a bit ambiguous. Notice that the thickness of the homogenized slab was taken to be equal to $d=N_L a$, apparently with good results. Next, to test if this choice still yields accurate results for very thin slabs, the reflection coefficient is computed for the same structure, except that now the slab has only one layer of rods ($N_L=1$). The reflection coefficient is depicted in Fig. 8 and has a peak at $k_y a=1.0$, which corresponds to the transition between propagating waves and evanescent waves. As seen, even though the slab is so thin the agreement is still remarkably good. This is a bit surprising, because for such a thin slab one would expect that the interface effects and granularity of the artificial medium would prohibit the homogenization of the structure using the bulk medium average fields.

In the next example, we study what happens if the angle of incidence φ is kept constant ($\varphi=45^\circ$), and the frequency is varied. Now $R=0.01a$, $N_L=5$, and the permittivity follows the Drude model $\epsilon=1-\beta_m^2/\beta^2$ with plasma wave number $\beta_m a=12.0$ or $\beta_m a=80.0$. The calculated results are shown in Fig. 9. For relatively low frequencies the two sets of data agree very well, but as the frequency increases the agreement progressively deteriorates, since the long wavelength limit approximation is no longer valid. Notice that for relatively low frequencies the medium blocks the incident radiation because the rods effectively behave as perfectly conducting wires.

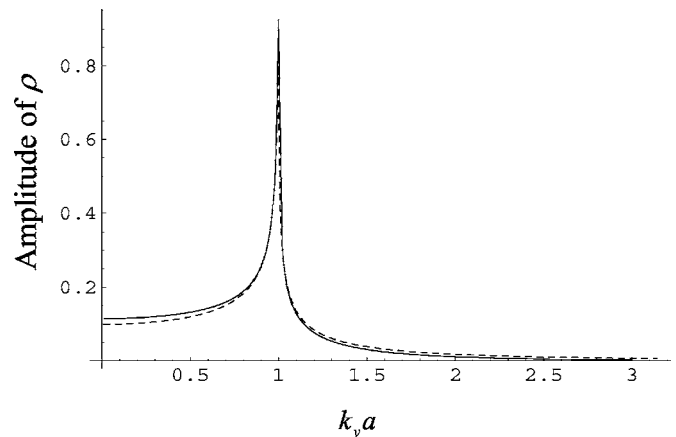


FIG. 8. Reflection coefficient as a function of $k_y a$ for $N_L=1$ layer, $R=0.05a$, and $\epsilon=-30$ at $\beta a=1.0$. The solid and dashed lines are defined as in Fig. 7.

So far the wave vector of the incident wave was always perpendicular to the axes of the ENG rods, and so the effects of spatial dispersion were hidden. In the last example, we consider the very different propagation scenario depicted in Fig. 6(b). The parameters of the rods are $R=0.05a$, $\epsilon=-30$, and $N_L=5$. The reflection coefficient for $\beta a=1.0$ is shown in Fig. 10 as a function of $k_z a$. Note that the angle of incidence θ for propagating waves satisfies $\sin \theta = k_z / \beta$. Figure 10 shows that the agreement between the numerical and analytical results is still quite satisfactory, except near the transition between the propagating waves and the evanescent waves ($k_z a \approx 1.0$).

It is important to refer that the configurations studied in this section (rods parallel to the interface) are not appropriate to achieve subwavelength imaging. For that application the rods must be perpendicular to the interface, as shown in Fig. 2(b). As discussed in Sec. IV, for this geometry three modes are excited in the (homogenized) rod medium, and thus an additional boundary condition is necessary to solve the scattering problem. The same situation occurs in the wire medium [15]. The analysis of this problem is out of the scope of this work and will be presented elsewhere.

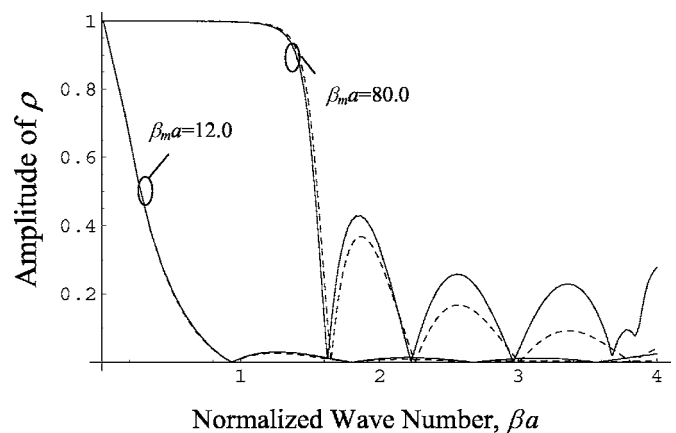


FIG. 9. Reflection coefficient as a function of the free-space wave number βa for $R=0.01a$, and $N_L=5$ layers. The permittivity of the rods follows a Drude-type model (see the text). The solid and dashed lines are defined as in Fig. 7.

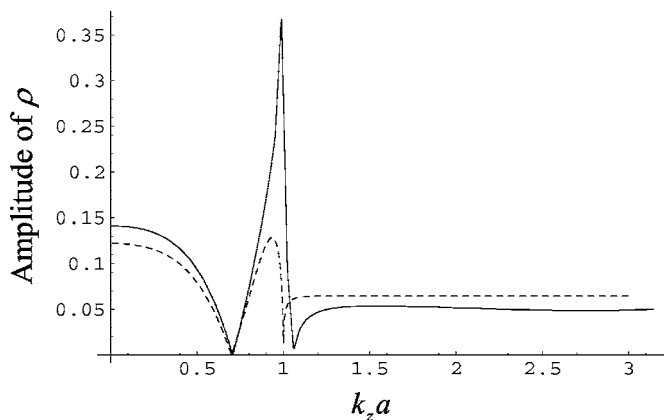


FIG. 10. Reflection coefficient as a function of $k_z a$ for the $N_L = 5$ layer, $R = 0.05a$, and $\epsilon = -30$ at $\beta a = 1.0$. The solid and dashed lines are defined as in Fig. 7.

VI. CONCLUSION

We studied the electrodynamics of a periodic array of thin ENG rods. Using the polarizability of a single rod and integral equation methods, we derived new nonlocal permittivity model for the artificial medium that accurately describes the propagation of waves in the long wavelength limit. We discussed the effects of spatial dispersion in the context of the reflection problem. It was proven that when the rods are parallel to interface only two modes (TE and TM) can be excited in the artificial medium. However, when the axes of the rods are normal to the interface, two TM modes, besides the TE mode, can be excited in the medium, as a manifestation of spatial dispersion. It was demonstrated that the wave normal contours of one of the TM modes are intrinsically hyperbolic. It was proven that the rod medium supports dispersionless modes that propagate along the axes of the rods, and it was speculated that this important property may allow subwavelength imaging of electromagnetic waves at the infrared and optical domains, using the idea proposed in [4]. It was shown that the energy of the dispersionless modes can be loosely bounded to the ENG rods (in this case the wave is essentially transverse electromagnetic), or alternatively tightly confined to a vicinity of the rods. In the latter case, the modes have approximately the same dispersion as the guided surface mode supported by an individual rod. The reflection problem was investigated in detail for the case where rods are parallel to the interfaces. The developed theory was successively tested against full wave data calculated with the MoM.

ACKNOWLEDGMENT

The author thanks Pavel A. Belov for valuable discussions.

APPENDIX A: DERIVATION OF THE MIXING FORMULA

In this Appendix we derive the mixing formula (13) used to homogenize the rod medium.

Let us consider a generic electromagnetic Floquet mode (\mathbf{E}, \mathbf{H}) , associated with the wave vector $\mathbf{k} = (k_x, k_y, k_z)$ and the wave number $\beta = \omega/c$, i.e., the fields satisfy Maxwell equations and $(\mathbf{E}, \mathbf{H})\exp(j\mathbf{k} \cdot \mathbf{r})$ is a periodic function in the lattice. The average electric field is defined as

$$\mathbf{E}_{\text{av}} = \frac{1}{V_{\text{cell}}} \int_{\Omega} \mathbf{E}(\mathbf{r}) e^{+j\mathbf{k} \cdot \mathbf{r}} d^3 \mathbf{r} \quad (\text{A1})$$

and \mathbf{H}_{av} is defined similarly. In the above, Ω represents the unit cell of the periodic medium. From the Maxwell equations it can be proven that

$$-\mathbf{k} \times \mathbf{E}_{\text{av}} + \beta \eta_0 \mathbf{H}_{\text{av}} = \mathbf{0}, \quad (\text{A2})$$

$$\beta \left(\mathbf{E}_{\text{av}} + \frac{\mathbf{P}}{\epsilon_0} \right) + \mathbf{k} \times \eta_0 \mathbf{H}_{\text{av}} = \mathbf{0}, \quad (\text{A3})$$

where the generalized polarization vector is given by

$$\frac{\mathbf{P}}{\epsilon_0} = \frac{1}{V_{\text{cell}}} \int_{\Omega} (\epsilon - 1) \mathbf{E} e^{+j\mathbf{k} \cdot \mathbf{r}} d^3 \mathbf{r}. \quad (\text{A4})$$

Straightforward calculations show that these relations imply that

$$\mathbf{E}_{\text{av}} = \frac{\beta^2 \bar{\mathbf{I}} - \mathbf{k} \mathbf{k}}{k^2 - \beta^2} \cdot \frac{\mathbf{P}}{\epsilon_0}. \quad (\text{A5})$$

The above equations are exact and completely general. Next we will apply these results to the rod medium under study. To begin with, we note that since the crystal is invariant to translations along the z direction the fields depend on z as $\exp(-jk_z z)$. Using standard Green's function methods [18], it can be proven that the electric field has the following integral representation,

$$\mathbf{E}(\mathbf{r}) = (\epsilon - 1) \int_S \beta^2 \bar{\mathbf{G}}_p(\mathbf{r}|\mathbf{r}') \cdot \mathbf{E}(\mathbf{r}') d^2 \mathbf{r}', \quad (\text{A6})$$

where the primed and unprimed coordinates represent the source and observation points, respectively, $S = \{(x', y', 0) : x'^2 + y'^2 \leq R^2\}$ is the cross section of the dielectric rod in the unit cell, and the Green's function dyadic is defined by

$$\bar{\mathbf{G}}_p = \left(\bar{\mathbf{I}} + \frac{1}{\beta^2} (\nabla_{\parallel} - jk_z \hat{\mathbf{u}}_z) (\nabla_{\parallel} - jk_z \hat{\mathbf{u}}_z) \right) \Phi_p. \quad (\text{A7})$$

In the above, $\Phi_p = \Phi_p(\mathbf{r}|\mathbf{r}')$ is the dynamic potential created by a phase-shifted array of line sources,

$$\nabla^2 \Phi_p + \beta^2 \Phi_p = - \sum_{\mathbf{I}} \delta(\mathbf{r}_{\parallel} - \mathbf{r}'_{\parallel} - \mathbf{r}_{\mathbf{I}}) e^{-j\mathbf{k} \cdot (\mathbf{r} - \mathbf{r}')}, \quad (\text{A8})$$

where δ is the Dirac function, $\mathbf{I} = (i_1, i_2)$ is a double index of integers, $\mathbf{r}_{\mathbf{I}} = a(i_1, i_2, 0)$ is a lattice point, and $\mathbf{r}_{\parallel} = (x, y, 0)$. Thus Φ_p is intrinsically two-dimensional, depending on z and z' as $e^{-jk_z(z-z')}$. Furthermore, it is obvious that the Green's function only depends on the relative position $\mathbf{r}_{\parallel} - \mathbf{r}'_{\parallel}$. Note that the Green's function can be written as a superposition of the potentials created by the line sources,

$$\Phi_p = \sum_{\mathbf{I}} \Phi_0(\mathbf{r}_{\parallel} - \mathbf{r}'_{\parallel} - \mathbf{r}_{\mathbf{I}}) e^{-j\mathbf{k} \cdot \mathbf{r}_{\mathbf{I}}}, \quad (\text{A9})$$

where $\Phi_0 = e^{-jk_z(z-z')} H_0^{(2)}(k_{\rho,0} |\mathbf{r}_{\parallel} - \mathbf{r}'_{\parallel}|) / 4j$ is the potential created by a line source placed at \mathbf{r}'_{\parallel} , i.e., the solution of Eq. (A8) when the summation in the right-hand side is restricted to the index $\mathbf{I}=\mathbf{0}$. Physically, Eq. (A6) establishes that the electric field at some point of space is the superimposition of the fields radiated by all the dielectric rods of the lattice.

The Green's potential can also be written as a Fourier series since it is a (pseudo) periodic function of the wave vector,

$$\Phi_p(\mathbf{r}|\mathbf{r}') = \frac{1}{A_{\text{cell}}} \sum_{\mathbf{J}} \frac{e^{-j\mathbf{k}_{\mathbf{J}} \cdot (\mathbf{r}-\mathbf{r}')}}{\mathbf{k}_{\mathbf{J}} \cdot \mathbf{k}_{\mathbf{J}} - \beta^2}, \quad (\text{A10})$$

where $A_{\text{cell}} = a^2$, $\mathbf{J} = (j_1, j_2)$ is a double index of integers, $\mathbf{k}_{\mathbf{J}} = \mathbf{k} + \mathbf{k}_{\mathbf{J}}^0$, and $\mathbf{k}_{\mathbf{J}}^0 = 2\pi a(j_1, j_2, 0)$.

Now that the necessary theoretical formalism was introduced, we are ready to study the homogenization problem in the rod medium. To begin with, we note that from Eqs. (A9) and (A10) that the Green's potential is singular in the spatial domain, i.e., when $\mathbf{r}_{\parallel} - \mathbf{r}'_{\parallel} \approx \mathbf{0}$ (source region), as well as in the spectral domain, i.e., when $\mathbf{k} \cdot \mathbf{k} \approx \beta^2$ (long wavelength limit). Since the integral (A6) is defined over the source region and we want to study the electromagnetic modes that propagate in the long wavelength limit, it is convenient to single out the terms that make the Green's function singular and decompose it as follows:

$$\Phi_p = \Phi_0 + \frac{1}{A_{\text{cell}}} \frac{e^{-j\mathbf{k} \cdot (\mathbf{r}-\mathbf{r}')}}{\mathbf{k} \cdot \mathbf{k} - \beta^2} + \Phi_{\text{reg}}, \quad (\text{A11})$$

where Φ_{reg} , which is defined implicitly by the above formula, is a regular function both in the spatial domain (source region $\mathbf{r}_{\parallel} - \mathbf{r}'_{\parallel} \approx \mathbf{0}$) and in the spectral domain (long wavelength limit). Using this decomposition in Eq. (A6) we find that

$$\begin{aligned} \mathbf{E}(\mathbf{r}) = & \mathbf{E}_{\text{av}} e^{-j\mathbf{k} \cdot \mathbf{r}} + (\varepsilon - 1) \int_S \beta^2 \bar{\bar{\mathbf{G}}}_0(\mathbf{r}|\mathbf{r}') \cdot \mathbf{E} d^2 \mathbf{r}' \\ & + (\varepsilon - 1) \int_S \beta^2 \bar{\bar{\mathbf{G}}}_{\text{reg}}(\mathbf{r}|\mathbf{r}') \cdot \mathbf{E} d^2 \mathbf{r}', \end{aligned} \quad (\text{A12})$$

where \mathbf{E}_{av} is the average field in the crystal, and $\bar{\bar{\mathbf{G}}}_0$ and $\bar{\bar{\mathbf{G}}}_{\text{reg}}$ are defined as $\bar{\bar{\mathbf{G}}}_p$, except that the Green's potential is replaced by Φ_0 and Φ_{reg} , respectively. To obtain the above result we used Eq. (A5). Next, we use the fact that the ENG rods are assumed to be very thin ($R/a \ll 1$), and that we want to investigate the electrodynamics of modes that propagate in the long wavelength limit ($|\mathbf{k}_{\parallel}|a \ll 2\pi$ and $\beta a \ll 2\pi$). Since the dyadic $\bar{\bar{\mathbf{G}}}_{\text{reg}}$ is regular in both the spatial and spectral domains, it is legitimate to write [putting $\mathbf{r}_{\parallel} = \mathbf{r}'_{\parallel} = \mathbf{0}$ and $\mathbf{k}_{\parallel} = (k_x, k_y, 0) = \mathbf{0}$],

$$\bar{\bar{\mathbf{G}}}_{\text{reg}}(\mathbf{r}|\mathbf{r}'; \mathbf{k}, \beta) \approx \bar{\bar{\mathbf{G}}}_{\text{reg}}(z|z'; k_z, \beta) \quad (\text{A13})$$

being the formula valid in the source region. For convenience, we introduce the following interaction dyadic:

$$\bar{\bar{\mathbf{C}}}_{\text{int}} = \beta^2 \bar{\bar{\mathbf{G}}}_{\text{reg}}(0; k_z, \beta). \quad (\text{A14})$$

Then, it is clear from Eq. (A12) that

$$\mathbf{E}(\mathbf{r}) \approx \left(\mathbf{E}_{\text{av}} + \bar{\bar{\mathbf{C}}}_{\text{int}} \cdot \frac{\mathbf{p}}{\varepsilon_0} \right) e^{-jk_z z} + (\varepsilon - 1) \int_S \beta^2 \bar{\bar{\mathbf{G}}}_0(\mathbf{r}|\mathbf{r}') \cdot \mathbf{E} d^2 \mathbf{r}' \quad (\text{A15})$$

provided the observation point \mathbf{r} is near the source region and $|\mathbf{k}_{\parallel}|a \ll 2\pi$. In above, we introduced the electric dipole moment (per unit of length), \mathbf{p} , of the dielectric rod in the unit cell. Now, the key result is that Eq. (A15) is formally equivalent to the (integral) equation obtained when a single rod is illuminated by a plane wave with electric field with amplitude $\mathbf{E}^{\text{inc}} = (\mathbf{E}_{\text{av}} + \bar{\bar{\mathbf{C}}}_{\text{int}} \cdot \mathbf{p} / \varepsilon_0)$ and the same wave vector component k_z along the z direction. In other words, when the rod in the unit cell stands alone in free space and is illuminated with the above defined plane wave, the total electric field also satisfies (to a first approximation) Eq. (A15) in the source region. But this remarkable result implies that

$$\frac{\mathbf{p}}{\varepsilon_0} = \bar{\bar{\alpha}}_e \cdot \left(\mathbf{E}_{\text{av}} + \bar{\bar{\mathbf{C}}}_{\text{int}} \cdot \frac{\mathbf{p}}{\varepsilon_0} \right), \quad (\text{A16})$$

where $\bar{\bar{\alpha}}_e$ is the electric polarizability tensor for a single rod. The term inside brackets in the right-hand side can be regarded as the local field that polarizes a single rod embedded in the dielectric crystal. Within the thin rod condition and for long wavelengths, the above solution is exact.

We are now ready to calculate the effective permittivity dyadic. Since the (macroscopic) electric displacement vector \mathbf{D} is given by $\mathbf{D} = \varepsilon_0 \mathbf{E}_{\text{av}} + \mathbf{p} / A_{\text{cell}}$, and the effective permittivity tensor must guarantee that $\mathbf{D} = \varepsilon_0 \bar{\bar{\varepsilon}} \cdot \mathbf{E}_{\text{av}}$, we conclude that the effective permittivity of the rod medium is given by the mixing formula (13). Note that (13) is completely general and is valid independently of the specific geometry of the transverse section of the rod.

At this point it is appropriate to compare (13) with the classic homogenization approach. It is striking that (13) reminds us of the Clausius-Mossotti formula [16,18]. Indeed, if we could identify the interaction dyadic $\bar{\bar{\mathbf{C}}}_{\text{int}}$ with $1/2A_{\text{cell}}$ the formulas would be the same (note also that the rods are arranged in a square lattice). In Appendix B we calculate the interaction dyadic in closed form using the static limit approximation. Equation (B4) shows that the interaction dyadic is different from $1/2A_{\text{cell}}$ only along the z direction. This important result shows that the Clausius-Mossotti formula is not valid for media with cylindrical inclusions. More specifically it fails to predict the effective permittivity along the direction in which the crystal is uniform. This is an indirect manifestation of spatial dispersion.

We also mention that the interaction dyadic defined by (A14) is not equivalent to the dynamic interaction constant defined in other works (see, for example [20]). Indeed, in our definition we extracted the singularities in both the spatial and spectral domains, while other works usually only extract the singularity in the spatial domain. It is clear from our previous analysis that it is the singularity in the spectral do-

main that indirectly defines the relation between the local field that polarizes the rod and the average field.

APPENDIX B: CALCULATION OF THE INTERACTION DYADIC

Here we calculate the interaction dyadic defined by Eq. (A14). It can be written as

$$\bar{\bar{C}}_{\text{int}} = (\beta^2 \bar{\bar{I}} + (\nabla_{\parallel} - jk_z \hat{\mathbf{u}}_z)(\nabla_{\parallel} - jk_z \hat{\mathbf{u}}_z))\Phi_{\text{reg}}, \quad (\text{B1})$$

where the right-hand side of the expression is evaluated at $\mathbf{r}=\mathbf{r}'=\mathbf{0}$ and $\mathbf{k}_{\parallel}=\mathbf{0}$. From Eqs. (A8) and (A11) it is clear that

$$\nabla^2 \Phi_{\text{reg}} + \beta^2 \Phi_{\text{reg}} = \left(\frac{1}{A_{\text{cell}}} - \sum_{\mathbf{I} \neq \mathbf{0}} \delta(\mathbf{r}_{\parallel} - \mathbf{r}'_{\parallel} - \mathbf{r}_{\mathbf{I}}) \right) e^{-j\mathbf{k} \cdot (\mathbf{r} - \mathbf{r}')}. \quad (\text{B2})$$

Putting $\mathbf{r}=\mathbf{r}'=\mathbf{0}$ and $\mathbf{k}=\mathbf{0}$ in the above equation, and letting β approach zero (static limit), we find that

$$\nabla^2 \Phi_{\text{reg}}(\mathbf{r}=\mathbf{r}'=\mathbf{0}; \mathbf{k}=\mathbf{0})|_{\beta=0} = \frac{1}{A_{\text{cell}}}. \quad (\text{B3})$$

Moreover, because of the symmetry of the square lattice it is evident that if $\mathbf{r}=\mathbf{r}'=\mathbf{0}$ and $\mathbf{k}=\mathbf{0}$ the following relations hold: $\frac{\partial^2 \Phi_{\text{reg}}}{\partial x_i \partial x_j} = 0$ if $i \neq j$, $\frac{\partial^2 \Phi_{\text{reg}}}{\partial z^2} = 0$, and $\frac{\partial^2 \Phi_{\text{reg}}}{\partial x^2} = \frac{\partial^2 \Phi_{\text{reg}}}{\partial y^2}$. So using Eq. (B3), we conclude that in the static limit ($\mathbf{k}=\mathbf{0}$ and $\beta=0$) the interaction dyadic is given by

$$\bar{\bar{C}}_{\text{int}} = \frac{1}{2A_{\text{cell}}} (\bar{\bar{I}} - \hat{\mathbf{u}}_z \hat{\mathbf{u}}_z). \quad (\text{B4})$$

The above result is consistent in the x - y plane with the (two-dimensional version of the) Clausius-Mossotti formula. However, along the z direction, maybe a bit surprisingly, the interaction constant vanishes in the static limit. Next, we will estimate $C_{\text{int},zz}$ in the dynamic case. From Eq. (B1), we have that

$$C_{\text{int},zz} = (\beta^2 - k_z^2) \Phi_{\text{reg}}. \quad (\text{B5})$$

Using Eqs. (A9) and (A11), and putting $\mathbf{r}=\mathbf{r}'=\mathbf{0}$ and $\mathbf{k}_{\parallel}=\mathbf{0}$, we obtain that

$$C_{\text{int},zz} = (\beta^2 - k_z^2) \sum_{\mathbf{I} \neq \mathbf{0}} \frac{1}{4j} H_0^{(2)}(k_{\rho,0} |\mathbf{r}_{\mathbf{I}}|) + \frac{1}{A_{\text{cell}}}. \quad (\text{B6})$$

The series in the right-hand side was evaluated in [14]. Using the results of [14], and assuming that $k_{\rho,0} a \ll \pi$, we obtain

$$C_{\text{int},zz} \approx k_{\rho,0}^2 \left(\frac{j}{4} + \frac{1}{2\pi} \ln \left(\frac{k_{\rho,0} a}{4\pi} \right) + \frac{C}{2\pi} + \frac{1}{12} + \sum_{n=1}^{\infty} \frac{1}{\pi |n|} \frac{1}{e^{2\pi|n|} - 1} \right), \quad (\text{B7})$$

where C is the Euler constant.

-
- [1] V. Veselago, *Sov. Phys. Usp.* **10**, 509 (1968).
[2] R. A. Shelby, D. R. Smith, and S. Schultz, *Science* **77**, 292 (2001).
[3] J. B. Pendry, *Phys. Rev. Lett.* **85**, 3966 (2000).
[4] P. A. Belov, C. R. Simovski, and P. Ikonen, *Phys. Rev. B* **71**, 193105 (2005).
[5] P. A. Belov, Y. Hao, and S. Sudhakaran, *Phys. Rev. B* **73**, 033108 (2006).
[6] C. Poulton, S. Guenneau, and A. B. Movchan, *Phys. Rev. B* **69**, 195112 (2004).
[7] A. L. Pokrovsky, *Phys. Rev. B* **69**, 195108 (2004).
[8] A. L. Pokrovsky and A. L. Efros, *Phys. Rev. Lett.* **89**, 093901 (2002).
[9] A. L. Pokrovsky and A. L. Efros, *Phys. Rev. B* **65**, 045110 (2002).
[10] P. A. Belov, R. Marques, S. I. Maslovski, I. S. Nefedov, M. Silveirinha, C. Simovski, and S. A. Tretyakov, *Phys. Rev. B* **67**, 113103 (2003).
[11] M. Silveirinha and C. A. Fernandes, *IEEE Trans. Microwave Theory Tech.* **53**, 1418 (2005).
[12] C. R. Simovski and P. A. Belov, *Phys. Rev. E* **70**, 046616 (2004).
[13] M. Silveirinha and C. A. Fernandes, *IEEE Trans. Antennas Propag.* **53**, 59 (2005).
[14] P. Belov, S. Tretyakov, and A. Viitanen, *J. Electromagn. Waves Appl.* **16**, 1153 (2002).
[15] M. Silveirinha, *IEEE Trans. Antennas Propag.* (to be published); cond-mat/0509612 (2005).
[16] A. Sihvola, *Electromagnetic Mixing Formulas and Applications*, IEE Electromagnetic Waves Series 47 (1999).
[17] J. Takahara, S. Yamagishi, H. Taki, A. Morimoto, and T. Kobayashi, *Opt. Lett.* **22**, 475 (1997).
[18] R. Collin, *Field Theory of Guided Waves* (IEEE, Piscataway, 1990).
[19] T. Wu, *Frequency-Selective Surface and Grid Array* (Wiley, New York, 1995).
[20] P. A. Belov and C. R. Simovski, *Phys. Rev. E* **72**, 026615 (2005).
[21] I. S. Nefedov, A. J. Viitanen, and S. A. Tretyakov, *Phys. Rev. E* **71**, 046612 (2005).